EPJ Photovoltaics **13**, 25 (2022)

https://doi.org/10.1051/epjpv/2022024

Available online at:
www.epj-pv.org

Special Issue on 'WCPEC-8: State of the Art and Developments in Photovoltaics', edited by Alessandra Scognamiglio, Robert Kenny, Shuzi Hayase and Arno Smets

REGULAR ARTICLE OPEN ACCESS

Ultra-lightweight and flexible inverted metamorphic four junction solar cells for space applications

Malte Klitzke[1,*], Jonas Schön[1,2], Rosalinda H. Van Leest[3], Gunther M.M.W. Bissels[3], Elias Vlieg[3,4], Michael Schachtner[1], Frank Dimroth[1], and David Lackner[1]

[1] Fraunhofer Institute for Solar Energy Conversion ISE, Heidenhofstr. 2, 79110 Freiburg im Breisgau, Germany
[2] INATECH – University of Freiburg, Emmy-Noether-Straße 2, 79110 Freiburg im Breisgau, Germany
[3] tf2 devices, Heyendaalseweg 135, 6525 AJ Nijmegen, The Netherlands
[4] Institute for Molecules and Materials, Radboud University, Heyendaalseweg 135, 6525 Nijmegen, The Netherlands

Received: 29 July 2022 / Received in final form: 26 September 2022 / Accepted: 20 October 2022

Abstract. In this work an inverted metamorphic four junction (IMM4J) solar cell with 30.9% conversion efficiency in beginning of life conditions under the AM0 (1367 W/m^2) spectrum is presented. Additionally, our newest improved IMM3J cell, consisting of $Ga_{0.51}In_{0.49}P/GaAs/Ga_{0.73}In_{0.27}As$ subcells, with 30.6% efficiency is also shown. The IMM4J solar cells consist of $Al_{0.05}Ga_{0.46}In_{0.49}P/Al_{0.14}Ga_{0.86}As/Ga_{0.89}In_{0.11}As/Ga_{0.73}In_{0.27}As$ subcells and are epitaxially grown by metal organic vapor phase epitaxy (MOVPE) on a GaAs substrate. These IMM solar cells achieve power-to-mass ratios of 3 W/g or more, which is more than three times higher than standard germanium based triple or four junction space solar cells. The losses in comparison to the simulated near-term potential efficiency of 33.8% for the IMM4J are analyzed in detail. Furthermore, the irradiation behavior for 1 MeV electron fluences of 1×10^{14} e^-/cm^2 and 2.5×10^{14} e^-/cm^2 for the IMM4J cells was investigated. A roadmap to further develop this concept towards an IMM5J with a realistic begin of life (BOL) efficiency potential of 35.9% under AM0 is presented.

Keywords: MOVPE / space solar cell / multi junction solar cell / end of life / photovoltaics

1 Introduction

Solar cells made of III-V semiconductor materials are typically used in space applications because, in addition to a high radiation tolerance [1], they also show the highest possible efficiencies. A direct wafer bonded five junction solar cell from Spectrolab demonstrated already a conversion efficiency of 36.0% [2]. A wafer bonded based four junction solar cell from Fraunhofer ISE showed an efficiency of 35.2% under AM0 conditions [3]. Recently, NREL presented an inverted metamorphic triple-junction cell with an middle cell absorber that includes a GaInAs/GaAsP superlattice with an efficiency of 34.2% under the AM0 reference spectrum [4]. Typical commercial available space solar cells from Spectrolab, Solaero and Azur Space [5–7] show efficiencies above 31% under the AM0 spectrum at begin of life.

Increasing number of missions with satellites employing electric propulsion systems and ever-increasing data volumes to be processed on satellites leading to a steady increase of the energy demand for e.g. communication satellites in geo-stationary orbits. At the same time, a reduction in mission launch cost is an important design goal of satellite manufacturers and operators today. Thin, flexible solar modules are an interesting option to fulfill these requirements, by maximizing the power-to-mass ratio and minimizing the stowage volumes [8]. Suitable thin, flexible solar cells with a high power to mass ratio are often realized by an inverted metamorphic multijunction solar cell structure and have already been demonstrated [9–12]. Such cells are grown in an inverted fashion: the highest bandgap subcell first, and the lowest bandgap subcell last. After the growth, the substrate is removed in a non-destructive manner by applying the Epitaxial Lift-Off (ELO) process that was used to manufacture the IMM3J solar cells [11]. The ELO process separates the IMM layer structure from the substrate by selectively etching away a thin intermediate AlAs release layer, without damaging the IMM layer structure nor the substrate [12,13]. This enables multiple reuses of the substrate which results in considerable savings in costs and precious raw materials. After the substrate removal, thin film processing is used to produce ultra-thin and thus also ultra-light flexible solar cells with a high power-to-mass ratio (>3 W/g), while maintaining

* e-mail: malte.klitzke@ise.fraunhofer.de

high efficiencies. Sharp demonstrated IMM3J solar cells with a design optimized for 1 MeV electron irradiation fluences with 1×10^{15} e^-/cm^2 which showed end of life efficiencies of 26.5% [10].

In general, increasing the number of subcells and spreading the range of bandgap energies is a key towards increasing solar cell conversion efficiencies. Progressing from an IMM triple to a quadruple junction can be done in two ways, either by adding a lower bandgap energy (<1.0 eV) bottom GaInAs cell together with an extended metamorphic buffer due to the higher lattice mismatch or by adding a higher bandgap energy (>1.9 eV) top cell by increasing the aluminum content in AlGaInP. The BOL efficiency potential of the lower bottom bandgap energy concept is slightly higher compared to the higher top bandgap energy IMM4J design. However, the lower bottom bandgap concept has several disadvantages: It is less irradiation hard due to the additional GaInAs subcell [14], it operates at higher temperatures due to the higher absorption in the wavelength range from 1200 nm to 1600 nm and this concept significantly increases the epitaxial layer thickness to overcome the lattice mismatch, which leads to longer and more expensive epitaxy processes. In order to minimize the epitaxy thickness and to avoid the other disadvantages, in this work the maximum lattice mismatch to the GaAs substrate and thus the composition of the bottom subcell was kept at $Ga_{0.73}In_{0.27}As$. In other words, the bottom cell bandgap was kept at about 1 eV while the top subcell bandgap was raised by 50 meV. The potential near term efficiency of this IMM4J design is 33.8% according to realistic simulations, which is already $3\%_{abs}$ higher than the realistic potential of the IMM3J. It will be shown, how this IMM concept can be further developed by increasing the top subcell bandgap to 2.10 eV while keeping the bottom subcell bandgap constant at 1.0 eV. This finally leads to an IMM5J solar cell with a realistic efficiency potential of 35.9% (AM0, BOL). We consider this the most cost-effective approach to increase the efficiency of IMM solar cells, since it minimizes the increase in epitaxial layer thickness. The suggested solar cell structures are schematically displayed in Figure 1.

2 Methods

The inverted grown metamorphic four junction cells (IMM4J) presented in this paper consist of $Al_{0.05}Ga_{0.46}In_{0.49}P$/$Al_{0.14}Ga_{0.86}As$/$Ga_{0.89}In_{0.11}As$/$Ga_{0.73}In_{0.27}As$ absorber materials whereby the two top cells are lattice matched to GaAs and for each of the metamorphic GaInAs sub-cells a step graded GaInP buffer is used to adjust the lattice constant (see Fig. 2 for a schematic sketch of the layer structure). The absorber materials and their thicknesses were chosen to attempt current matching at begin of life (BOL) conditions under the AM0 (1367 W/m^2) reference spectrum. Due to the early development stage, as it will be shown below, the target of current matching under BOL conditions was not fully reached yet. Close to fully transparent tunnel diodes are located between the subcells to allow a series connection of all junctions. In Figure 2 each junction and both metamorphic buffers are shown on the lattice constant versus bandgap plot for III-V semiconductors. An etchstop layer stack is located prior to the first junction to allow subsequent removal of the substrate. The complete structure has a total thickness of 13 μm and was realized by metal organic vapor phase epitaxy (MOVPE) in an AIXTRON 2800G4-TM planetary reactor in an $8 \times 4''$ configuration. The details to the growth of previous generations of IMM3J solar cells and to the full two dimensional opto-electrical model simulations can be found in Schön et al. [11].

A thin metal layer stack is applied on top of the epitaxial layers directly after the growth, which serves as mirror for the bottom cell (J4) and as a backside contact for the entire multijunction solar cell. After the substrate removal, the metal layer stack further serves as a mechanical carrier for the ultra-thin epitaxial layers. The substrate removal was realized in this case by etching away the GaAs substrate. The resulting thin-films were subsequently processed into thin-film IMM solar cells using standard lithography, metallization and wet chemical etching processes. In addition, an anti-reflection coating of ZnS/MgF_2 was applied by thermal evaporation. The fully processed thin-film IMM4J solar cells were weighted with a laboratory weight scale and reached very low areal mass densities of 14 mg/cm^2. All wafer removal and thin-film processing steps were carried out by tf2 devices in Nijmegen, the Netherlands.

For the analyses and optimization of the solar cells, numerical simulations were carried out. Two-dimensional opto-electrical models of the different 4J and 5J cell designs were elaborated in Sentaurus TCAD [15] based on the model for the IMM3J end of life (EOL) solar cell [11]. The optical model is based on the Transfer-Matrix Method, while the charge carrier transport, tunnel processes and recombination are considered in the electrical part. Material properties and models for GaInP, GaInAs and AlGaAs were taken from previous studies [11] and the optical and electrical parameters for AlGaInP were extracted from measurements at single junction solar cells. For ternary materials with varying compositions the optical material parameters were generated by using a morphing algorithm presented in reference [16]. For an estimate of realistic efficiency potentials that are reachable with the available material quality, simulations were carried out with Shockley-Read-Hall lifetimes extracted from former measurements on inverted grown samples. We use smaller electron lifetimes for the AlGaInP base, namely 1 ns (1.95 eV) down to 0.5 ns (2.10 eV) compared to the $Ga_{0.51}In_{0.49}P$ base (1.4 ns [11]).

Calibrated characterization under an AM0 (1367 W/m^2) reference equivalent spectrum and external quantum efficiency measurements of every subcell of the IMM cells were conducted at the CalLab Fraunhofer ISE with adjustable multi-source sun simulators [17,18]. The IMM4J solar cells were sent to TU Delft for 1 MeV electron irradiation. Half of the cells received a fluence of 1×10^{14} e^-/cm^2 and the second half received a fluence of 2.5×10^{14} e^-/cm^2 to simulate typical doses expected for low earth orbit missions. The irradiated cells were treated with a subsequent annealing according to the ECSS standard [19] by being exposed to the AM0

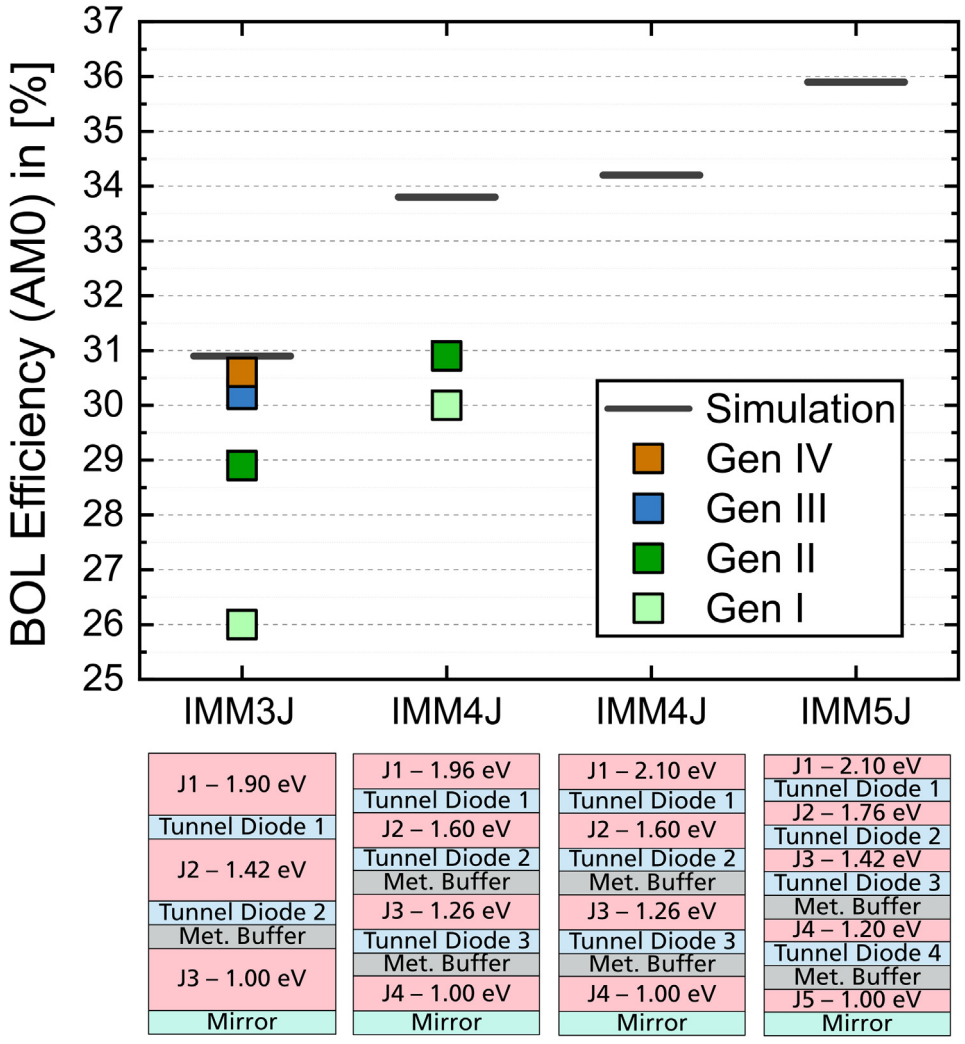

Fig. 1. Development steps from an IMM 3J solar cell towards an IMM5J solar cell with BOL design. For comparison, the simulated near-term efficiency potential and the already achieved efficiencies for the IMM3J and IMM4J are shown. Keep in mind that the IMM3J is optimized for EOL conditions, whereas the 4J and 5J structures for BOL. The sketch of the layer structure shows schematically that increasing the number of junctions is not increasing the total epitaxy thickness heavily. Note that for an IMM4J cell with top subcell bandgap up to 2.1 eV, all other absorber material bandgap energies stay the same.

spectrum for 48 h and then being kept at an elevated temperatures of 60 °C for 24 h. IV curves, EQEs and spectral electroluminescence were again measured on the irradiated cells after the annealing. Subcell open circuit voltages were determined using the reciprocity relation described in [20] with calibrated external quantum efficiency and spectral electroluminescence measurement data of the IMM4J solar cells. Handling during characterization, shipping, and irradiation was done as carefully as possible using standard tweezers and equipment, but still the many steps resulted in cracks and defects (see Fig. 3) in the thin film solar cells. To obtain more reliable data, the cells must be mounted on temporary substrates immediately after processing and weight measurements.

3 Results and discussion

3.1 Begin of life

The newest generation (Gen IV) of IMM3J solar cells reached an efficiency of 30.6% (AM0, BOL) with a fill factor of 83%, a J_{sc} of 16.5 mA/cm^2 and a V_{oc} of 3.06 V. The efficiency gain compared to the former solar cells presented in reference [11] is mainly caused by an improved current matching and thus higher J_{sc}. In Figure 4 the light IV curve of the Gen IV of IMM3J is shown together with the IV curves for the first and second generations of IMM4J solar cells. For comparison purpose the simulation targets of the IMM3J and IMM4J are shown.

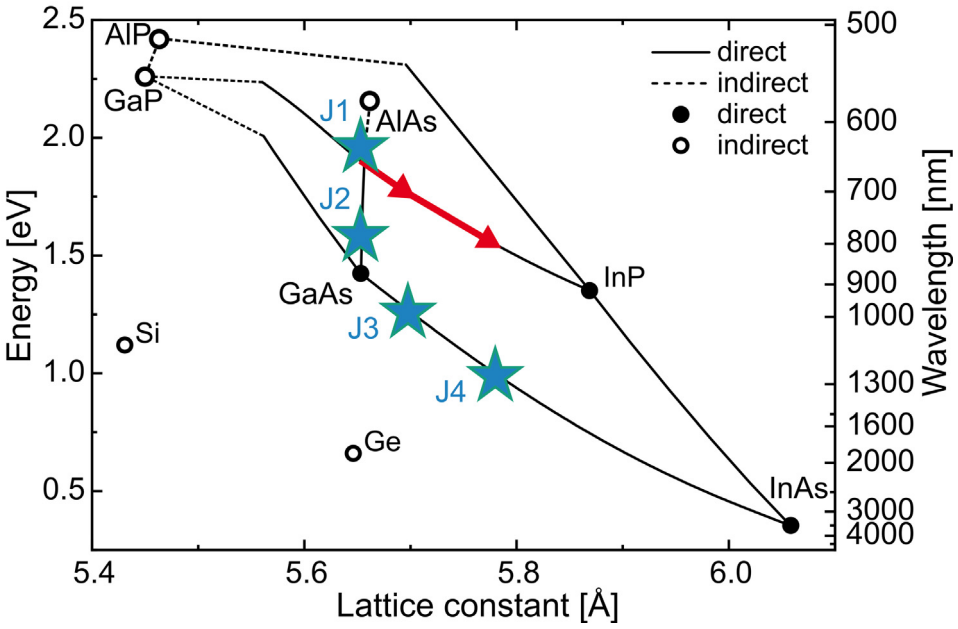

Fig. 2. Lattice constant vs. bandgap energy plot of III-V semiconductors. The four different absorber materials used in the IMM4J are marked as blue stars and the two GaInP step-graded metamorphic buffers are marked as red arrows. J1 is the $Al_{0.05}Ga_{0.46}In_{0.49}P$, J2 is the $Al_{0.14}Ga_{0.86}As$, J3 is the $Ga_{0.89}In_{0.11}As$ and J4 is the $Ga_{0.73}In_{0.27}As$ cell.

The first generation of the IMM4J reached already 30% efficiency under the AM0 reference spectrum and the second generation of IMM4J exceeds the newest generation of IMM3J with an efficiency of 30.9% a fill factor of 82.8%, a J_{sc} of 12.55 mA/cm^2 and a V_{oc} of 4.07 V. Gen I was current limited by subcell 4 and suffered additionally from a relatively low fill factor of 81.1% (see Fig. 4). The current limiting subcell (J4) of this cell has likely a low parallel resistance which explains the significantly lower than expected fill factor. In Gen II the current matching and thus the J_{sc} (12.55 mA/cm^2) was improved. The current is now limited by subcell 2 (see Fig. 5) which led to an increased FF (see Fig. 4). However, the current matching can be improved further in following generations. Just by adjusting the absorber thickness of the subcells, the next generation could achieve already a J_{sc} of 12.9 mA/cm^2, which is very close to the near-term potential predicted by simulation of 13.0 mA/cm^2. Further, the EQE plot (Fig. 5) reveals a current loss of approximately 0.3 mA/cm^2 in the Gen II compared to the simulation (gray, dashed line). To determine whether this is due to parasitic absorption in the tunnel diode or recombination in the AlGaAs emitter is the target of current investigations.

Additionally, the V_{oc}, which is correlated to the material quality, is already close to the simulated values (see Fig. 4) and therefore the main improvement potential for the IMM4J is in the fill factor. The fill factor could be improved by avoiding handling caused cracks and shunts (see EL images in Fig. 3) in the thin film devices [11] and by lowering the series resistance (R_s). The difference in slopes around V_{oc} between the simulation and the Gen II device suggests the FF loss to be dominated by the series resistance. Measurements of Gen I IMM3J solar cells at different temperatures (not shown) reveal that this resistor has probably a lower temperature sensitivity as expected from an ohmic type resistor. The root cause of this unexpected high series resistance is still under investigation.

The subcell open circuit voltages were determined from spectral electroluminescence data. The resulting values for the Gen II IMM4J in BOL and after electron irradiation (see Sect. 3.2) are shown together with the results from the latest generation of IMM3J for comparison in Figure 6. The detailed balance limit for the V_{oc} as a function of bandgap is shown together with a 123 mV downshifted curve, which serves as guide for the eye for equal absorber material expectations. In BOL condition J2 shows by far the highest material quality and reaches a similar voltage difference to the detailed balance limit as the GaAs middle cell in the IMM3J. The $Al_{0.05}Ga_{0.46}In_{0.49}P$ absorber shows a slightly lower quality as the $Ga_{0.51}In_{0.49}P$ cell in the IMM3J but nevertheless the higher bandgap allows a gain in V_{oc} by about 40 mV. The difference of the shifted detailed balance limit line to the V_{oc} values of the metamorphic GaInAs subcells suggest, that the largest improvement of the BOL V_{oc} can be achieved by improving the growth and design of especially J3. W_{OC} (E_g/e - V_{oc}) values of 410 mV have been already demonstrated in literature [21] for such metamorphic GaInAs cells. Thus, a V_{oc} increase of about 30 mV in J3 and of about 20 mV in J4 seems possible in future developed devices. Improvements of the current matching, fill factor and W_{OC} will lower the difference to the simulation target in following generations. Compared to the IMM3J device these improvements would lead not only

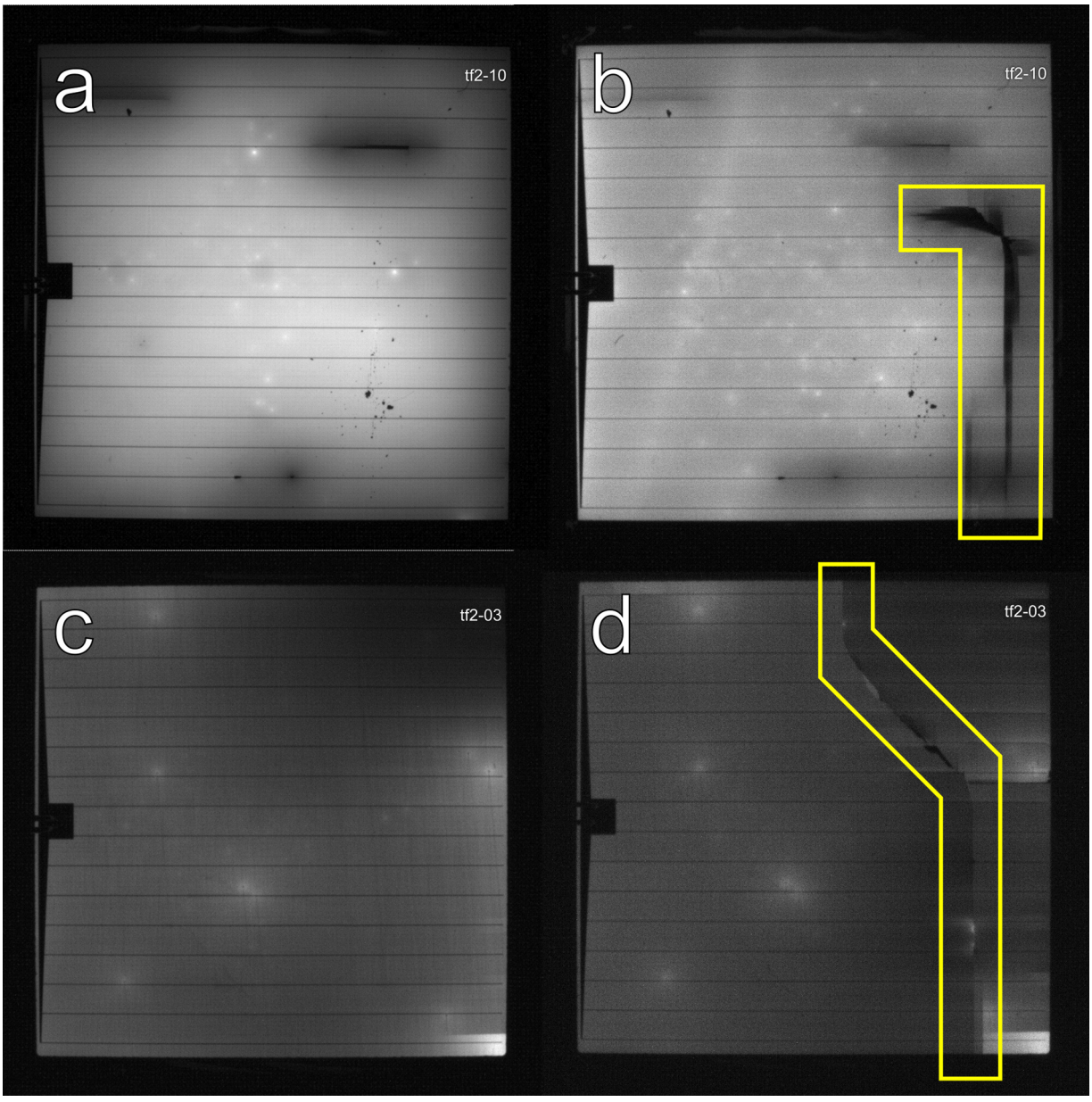

Fig. 3. Spatial electroluminescence measurements of two IMM4J solar cells before (a & c) and after (b & d) electron irradiation. In all four images a few shunts (bright spots) are observable and after electron irradiation huge cracks (yellow marking) were formed due to the amount of handling step of this thin film devices.

to an efficiency gain but also to a higher power-to-mass ratio, since the increase in weight and thickness from IMM3J to IMM4J is negligible.

In Figure 1 our roadmap towards an IMM5J with a simulated BOL efficiency of 35.9% assuming current material qualities is shown together with the measured and simulated near-term potential efficiencies of the different development stages of our IMM3J and IMM4J solar cells. The bottom subcell is in all cases kept at a bandgap of 1.00 eV, keeping the maximum lattice mismatch to the GaAs substrate and the absorber material composition ($Ga_{0.73}In_{0.27}As$) constant for all the presented IMM designs. This allows the usage of the same metamorphic step graded buffers to reach the required lattice constants for the metamorphic bottom subcells. Therefore, the total epitaxial growth thickness and growth time is only minimally increased with increasing number of junctions. This allows similar areal mass densities of 11.27 mg/cm^2 as already demonstrated by the Gen IV of IMM3J for all the IMM solar cells designs presented in this work. The simulated near-term potential efficiency (34.2%) of the IMM4J solar cell design with a 2.10 eV top subcell is plotted in Figure 7 with the areal mass density of the Gen IV IMM3J as current target for comparison.

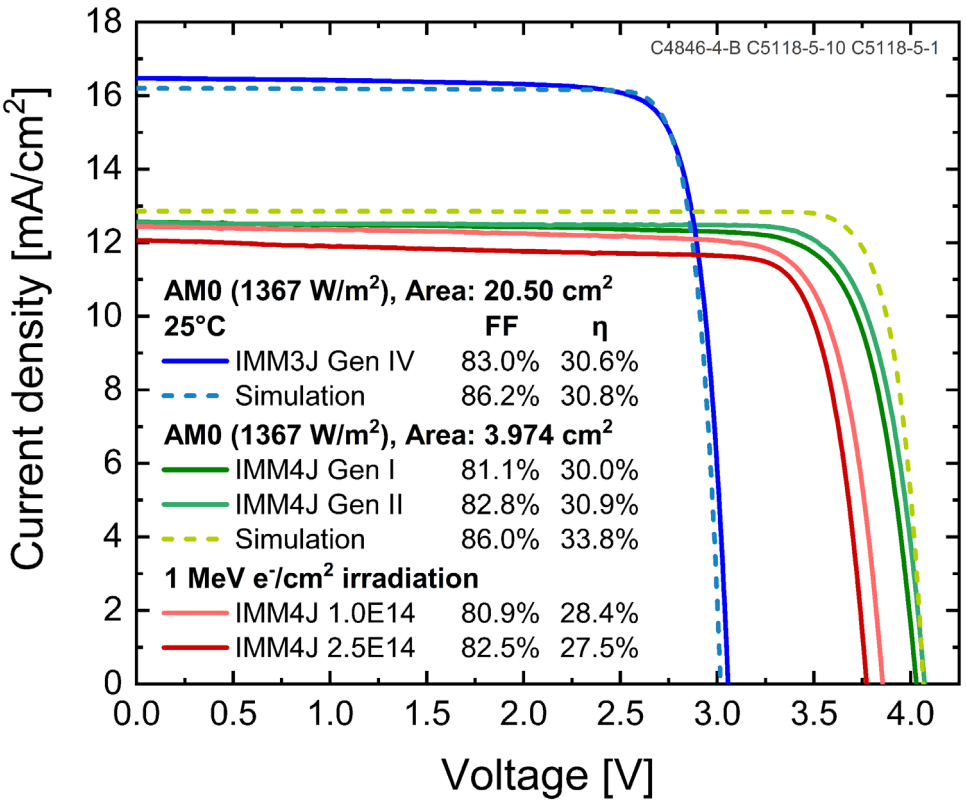

Fig. 4. Light IV curves for the first two generations of IMM4J solar cells in BOL condition (solid green). The light IV curve for the last generation of IMM3J in BOL condition is shown for comparison (solid blue). The simulated realistic potential IV curves for both devices are shown as dashed lines. IV curves of the best cells after 1 MeV electron irradiation with a fluence of 1×10^{14} e^-/cm^2 and 2.5×10^{14} e^-/cm^2 are shown in solid pink and red respectively.

3.2 After electron irradiation

The IMM4J solar cells from the second generation have been irradiated with 1 MeV electrons with a fluence of 1×10^{14} e^-/cm^2 and 2.5×10^{14} e^-/cm^2 to simulate typical missions in low earth orbits. The open circuit voltages after irradiation and subsequent annealing (as described in Sect. 2) are shown in Figure 8 in absolute comparison to the BOL values. The solar cells V_{oc} degrade after 1×10^{14} e^-/cm^2 on average by 220 mV and 270 mV after 2.5×10^{14} e^-/cm^2. In comparison, the IMM3J reported by Sharp (3100 mV, BOL) degrades in V_{oc} after a fluence of 2.5×10^{14} e^-/cm^2 by about 215 mV [10]. The higher loss in V_{oc} of the IMM4J after nominally the same fluences is caused due to the fact, that the IMM4J starts in BOL conditions already with very high V_{oc} values (4071 mV, BOL). In Figure 4 the light IV curves under AM0 illumination for the two best irradiated cells are shown. The degradation results in an efficiency of 28.4% after 1×10^{14} e^-/cm^2 and 27.5% after 2.5×10^{14} e^-/cm^2 fluences. The second generation of IMM4J solar cells was designed for high BOL efficiencies and thus suffer in comparison to references (see Fig. 7) stronger under the same irradiation fluences. To achieve higher efficiency potentials after irradiation the solar cell must be designed in a way that the radiation hardest subcell (i.e. the top cell) is the current limiting junction in non-irradiated conditions.

Subcell voltages for the irradiated IMM4J cells have been calculated as described already in Section 2 and are also plotted in Figure 6 in comparison to the corresponding BOL values. The arsenic based subcells all degraded in V_{oc} to approximately the same offset to the radiative limit, which means that already at this low irradiation dose, the minority carrier lifetime is strongly limited by the irradiation induced damage in those subcells. The phosphorus based top cell is the radiation hardest material in the IMM4J and is therefore only slightly degraded in V_{oc}. The $Al_{0.05}Ga_{0.46}In_{0.49}P$ top cell only loses 12 mV in V_{oc} after 2.5×10^{14} e^-/cm^2 fluence irradiation. More than half of the loss in V_{oc} (145 mV of 280 mV) in the IMM4J is related to the degeneration in the $Al_{0.14}Ga_{0.86}As$ subcell ($J2$) after the irradiation. The average subcell W_{OC} of the IMM4J degraded from 435 mV in BOL condition to 510 mV after 2.5×10^{14} e^-/cm^2.

The main approach of inverse grown metamorphic multijunction solar cells is to maximize the power-to-mass ratio without lowering the efficiency potential. In Figure 7 the power-to-mass ratios versus efficiencies of commercially available multijunction solar cells are compared to the presented IMM cells before and after irradiation. The solar cells based on direct growth on Germanium and subsequent substrate thinning show power-to-mass ratios slightly below 1 W/g. The IMM3J and IMM4J junction solar cells

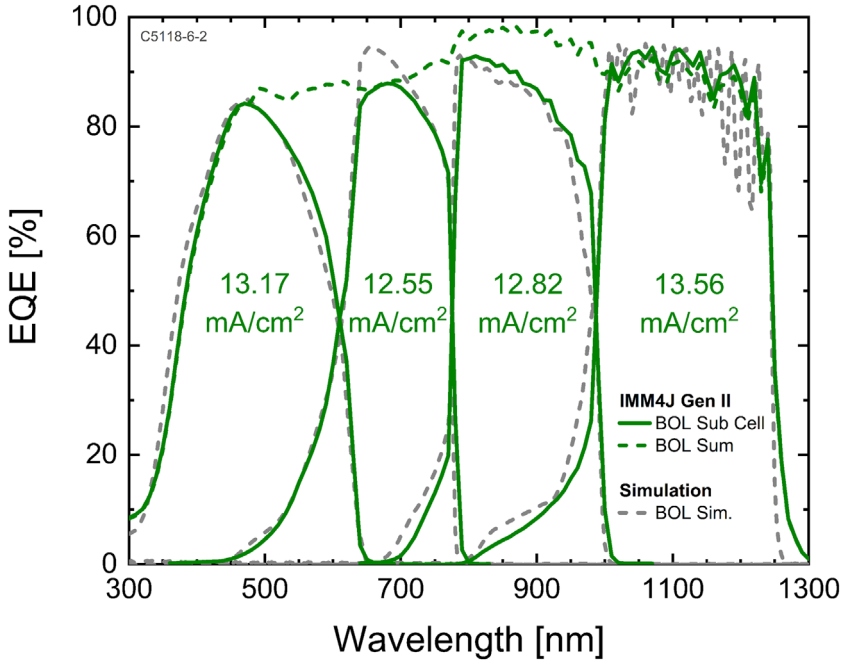

Fig. 5. Plot of the measured EQEs of each subcell (solid lines) and of the sum (dotted line) of a Gen II IMM4J solar cell. The dashed line represents the realistic near-term potential simulation of the subcell EQEs. Subcell current densities were calculated from the subcell EQEs for the case of the AM0 spectrum.

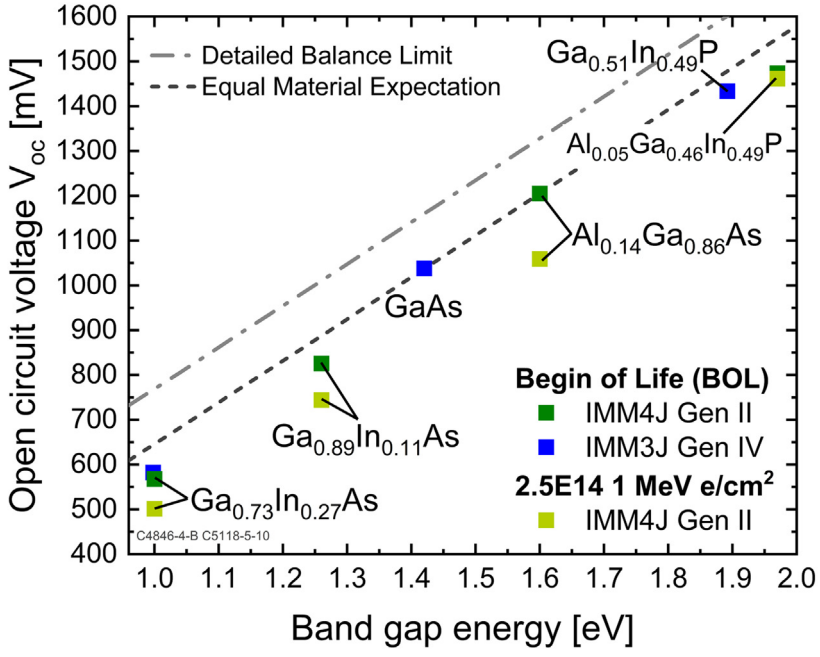

Fig. 6. From spectral electroluminescence measurements, IV data and measured quantum efficiencies calculated subcell open circuit voltages for the IMM4J before and after 2.5×10^{14} 1MeV e^-/cm^2 electron irradiation. The calculated subcell open circuit voltages for the latest generation of IMM3J are shown as comparison. The parallel curve (shifted downwards by 123 mV) to the radiative limit [23] serves as guide to the eye and can be interpreted as guide for equal material expectation.

presented in this work and literature data from Sharp [10] and MicroLink [22] show 3.5 to 4.5 times higher power-to-mass ratios while showing comparable efficiencies in BOL and soft irradiation conditions. For the latest generation of our IMM3J solar cell unfortunately no irradiation data is available yet, but from simulations and irradiation data from previous generations [11], it can be assumed that the cell will behave comparable to the IMM space solar cell

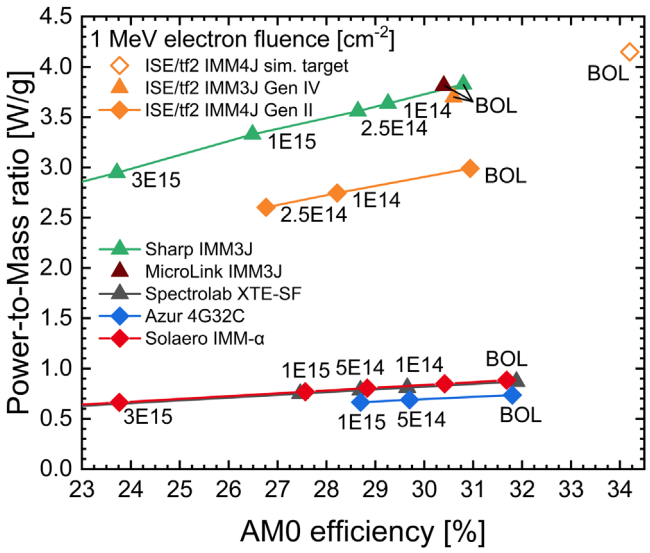

Fig. 7. AM0 power-to-mass ratios vs. efficiencies plot of the IMM4J and IMM3J in comparison to commercial available solar cells. 1 MeV electron irradiation fluences in e^-/cm^{-2} are labelled on the symbols to show the degeneration of each cell. For the latest generation of IMM3J are unfortunately no irradiation results available yet. The 4G32C from Azur [5] and the XTE-SF from Spectrolab [6] are based on thinned Germanium substrates whereas the cells from Sharp [10] and MicroLink [22] are IMM3J based solar cells. The IMM based solar cells have a more than three times higher power-to-mass ratio in comparison to the thinned Germanium based devices. The IMM-α from Solaero [7] is an IMM based solar cell but permanently bonded to a robust substrate and therefore not as lightweight as the other IMM based cells. The ISE/tf2 simulation target assumes an areal mass density of 11.27 mg/cm^2 (as for the Gen IV IMM3J) and the realistic efficiency potential of 35.9% of the IMM4J design with a bandgap spread from 2.10 eV to 1.00 eV.

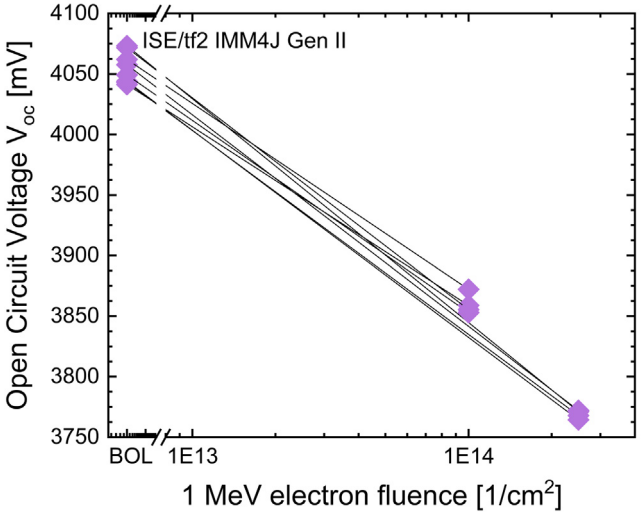

Fig. 8. The open circuit voltages for BOL and soft irradiation conditions of different IMM4J solar cells from the same MOVPE run. They degraded on average 220 mV after an irradiation with 1 MeV electrons after a fluence of 1×10^{14} e^-/cm^2 and about 270 mV after 2.5×10^{14} e^-/cm^2.

from Sharp [10]. Additionally, the spatial electroluminescence images (see Fig. 3) of the solar cells after irradiation indicate that more defects are introduced during the many intermediate handling steps with standard tweezers of the thin film devices. For more reliable irradiation data, the cells must be mounted on temporary substrates directly after processing and weight measurements.

4 Conclusion

We further improved the efficiency and power-to-mass ratio of our IMM3J solar cell compared to our previous publication [11] and reach an efficiency of 30.6%. The latest generation of our IMM3J optimized for EOL performance has a power-to-mass ratio of 3.7 W/g and shows the lightweight potential of these devices after full processing. The second generation of IMM4J solar cells already outperforms the latest generation of the IMM3J space solar cells with an efficiency of 30.9% under the AM0 spectrum. The simulated near-term target of the IMM4J solar cell with a bandgap spread from 1.96 eV to 1.00 eV is 33.8% and can realistically be achieved in following generations. This result is a steppingstone towards the realization of an IMM5J based on the same platform. The proposed IMM5J features a 2.10 eV top subcell and the same 1.00 eV bottom subcell, with a realistic efficiency potential of 35.9%. The IMM solar cells show a very high power-to-mass ratio over 3 W/g, which can be achieved by all designs presented in this work and outperform in this category the commercial available space solar cells based on thinned Germanium substrates by more than a factor of three. After electron irradiation, to simulate low earth orbit operations, the IMM4J solar cells optimized for BOL conditions showed 28.4% after a 1 MeV electron fluence of 1×10^{14} e^-/cm^2 and 27.5% after 2.5×10^{14} e^-/cm^2 in efficiency. The power-to-mass ratio of the current IMM4J generation in EOL condition is 2.6 W/g. This high power-to-mass ratio, the compatibility with flexible solar generators with very low stowage volumes and the possibility of growth substrate reuse by applying the ELO process can significantly reduce launch costs for satellites equipped with IMM based solar panels. Especially for earth low orbit missions this approach is a very attractive option in future missions.

Author contribution statement

M. Klitzke: AlGaInP top cell and epitaxy development, data analysis and interpretation, main manuscript writing.
J. Schön: Numerical simulations, feedback to manuscript.
R. H. Van Leest: Thin-film solar cell processing, Initial analysis.
G. M. M. W. Bissels: Funding acquisition contribution, feedback and corrections to manuscript, thin-film solar cell processing.
E. Vlieg: Supervision of tf2 contribution.
M. Schachtner: Characterization of multijunction solar cells in Fraunhofer ISE CalLab.
F. Dimroth: General advisor and contribution to the IMM-roadmap.
D. Lackner: IMM cell and epitaxy development, feedback to manuscript, supervision of ISE contribution.

For the operation and maintenance of the MOVPE reactor, the authors would like to thank the whole MOVPE team at Fraunhofer ISE and Dr. Jens Ohlmann, Sophie Zimmermann and Fadil Sahajad in detail. For the extensive and detailed cell characterizations the authors would like to acknowledge G. Siefer and E. Fehrenbacher. The authors would like to especially thank AZUR SPACE for organizing the electron irradiation at TU DELFT and subsequent annealing of the solar cells presented in this work. This work was supported by the European Space Agency ESA-ESTEC (contract No. 4000128123/19/NL/FE). The research leading to these results has received funding from the European Union's Horizon 2020 Research and Innovation Programme, under Grant Agreement no EU/821876. This work was also supported by the German Federal Ministry for Economic Affairs and Climate Action (BMWK) under the project "50Prozent" (BMWK, 03EE1060).

References

1. M. Yamaguchi, Radiation-resistant solar cells for space use, Solar Energy Mater. Solar Cells **68**, 31 (2001)
2. P.T. Chiu, D.C. Law, S.B. Singer et al., High performance 5J and 6J direct bonded (SBT) space solar cells, in *2015 IEEE 42nd Photovoltaic Specialist Conference (PVSC)*. (IEEE, 2015), pp. 1–3
3. G. Siefer, P. Beutel, D. Lackner et al., Four-junction wafer bonded solar cells for space applications, in *2019 European Space Power Conference (ESPC)*. (IEEE, 2019), pp. 1–4
4. R.M. France, J.F. Geisz, T. Song et al., Triple-junction solar cells with 39.5% terrestrial and 34.2% space efficiency enabled by thick quantum well superlattices, Joule **6**, 1121 (2022)
5. W. Guter, F. Dunzer, L. Ebel et al., Space solar cells – 3G30 and next generation radiation hard products, E3S Web Conf. **16**, 3005 (2017)
6. P.T. Chiu, D.C. Law, C.M. Fetzer et al., Qualification of 32% BOL and 28% EOL efficient XTE solar cells, in *2019 IEEE 46th Photovoltaic Specialists Conference (PVSC)*. (IEEE, 2019), pp. 1506–1509
7. D. Derkacs, D. Aiken, Z. Bittner et al., Development of IMM-α and Z4J radiation hard III-V solar cells, in *2018 IEEE 7th World Conference on Photovoltaic Energy Conversion (WCPEC)* (A Joint Conference of 45th IEEE PVSC, 28th PVSEC & 34th EU PVSEC). (IEEE, 2018), pp. 3757–3762
8. D. Vergnet, V. Khorenko, G. Bissels et al., Advanced lightweight flexible array with mechanical architecture, in *2019 IEEE 46th Photovoltaic Specialists Conference (PVSC)*. (IEEE, 2019), pp. 2808–2810
9. J.F. Geisz, S.R. Kurtz, M.W. Wanlass et al., Inverted GaInP/(In)GaAs/InGaAs triple-junction solar cells with low-stress metamorphic bottom junctions, in *2008 33rd IEEE Photovolatic Specialists Conference*. (IEEE, 2008), pp. 1–5
10. M. Imaizumi, T. Takamoto, N. Kaneko et al., Qualification test results of IMM triple-junction solar cells, space solar sheets, and lightweight & compact solar paddle, E3S Web. Conf. **16**, 3012 (2017)
11. J. Schön, G.M.M.W. Bissels, P. Mulder et al., Improvements in ultra-light and flexible epitaxial lift-off GaInP/GaAs/GaInAs solar cells for space applications, Progr. Photovolt. **30**, 1003 (2022)
12. J.J. Schermer, Method for separating a film and a substrate, US Patent 6,974,521 (2005)
13. G.J. Bauhuis, P. Mulder, J.J. Schermer, Thin-film III–V solar cells using epitaxial lift-off, in *High-Efficiency Solar Cells*, edited by X. Wang, Z.M. Wang (Springer International Publishing, Cham, 2014), Vol. 190, pp. 623–643
14. P. Patel, D. Aiken, A. Boca et al., Experimental results from performance improvement and radiation hardening of inverted metamorphic multijunction solar cells, IEEE J. Photovolt. **2**, 377 (2012)
15. T. Synopsys, Sentaurus: Sentaurus device user guide release H-2013.03 (2013)
16. P. Schygulla, P. Fuß-Kailuweit, O. Höhn et al., Determination of the complex refractive index of compound semiconductor alloys for optical device modeling, J. Phys. D: Appl. Phys. **53**, 495104 (2020)
17. M. Schachtner, R. Hoheisel, F. Sabuncuoglu et al., A new tool to measure monolithic multi junction solar cells with up to six subcells, in *26th European Photovoltaic Solar Energy Conference and Exhibition* (2011), pp. 199–204
18. G. Siefer, T. Gandy, M. Schachtner et al., Improved grating monochromator set-up for EQE measurements of multi-junction solar cells, in *2013 IEEE 39th Photovoltaic Specialists Conference (PVSC)*. (IEEE, 2013), pp. 86–89
19. ESA-ESTEC, ECSS-E-ST-20-08C Rev.1. European Cooperation for Space Standardization (2012), pp. 1–197
20. S. Roensch, R. Hoheisel, F. Dimroth et al., Subcell I–V characteristic analysis of GaInP/GaInAs/Ge solar cells using electroluminescence measurements, Appl. Phys. Lett. **98**, 251113 (2011)
21. J.F. Geisz, R.M. France, K.L. Schulte et al., Six-junction III–V solar cells with 47.1% conversion efficiency under 143 Suns concentration, Nat. Energy **5**, 326 (2020)
22. D. Cardwell, A. Kirk, C. Stender et al., Very high specific power ELO solar cells (>3 kW/kg) for UAV, space, and portable power applications, in *2017 IEEE 44th Photovoltaic Specialist Conference (PVSC)*. (IEEE, 2017), pp. 3511–3513
23. W. Shockley, H.J. Queisser, Detailed balance limit of efficiency of p-n junction solar cells, J. Appl. Phys. **32**, 510 (1961)

Cite this article as: Malte Klitzke, Jonas Schön, Rosalinda H. Van Leest, Gunther M.M.W. Bissels, Elias Vlieg, Michael Schachtner, Frank Dimroth, David Lackner, Ultra-lightweight and flexible inverted metamorphic four junction solar cells for space applications, EPJ Photovoltaics **13**, 25 (2022)